WELDING RESEARCH

SUPPLEMENT TO THE WELDING JOURNAL, AUGUST 1974

Sponsored by the American Welding Society and the Welding Research Council

# Inclusions and Susceptibility to Lamellar Tearing of Welded Structural Steels

*The role of inclusions in lamellar tearing has been investigated and the important types and critical quantitative parameters have been identified*

BY J. C. M. FARRAR

## Introduction

Lamellar tearing is a world wide problem in the fabrication of structural and pressure vessel steelwork. Significant steps have been taken in the past few years to provide information which will enable designers to avoid the occurrence of the problem, and a number of precautionary and remedial techniques are available for the welding engineer (Refs. 1-3). In addition it has been shown that good correlations exist between susceptibility to cracking in practice and the results of small scale mechanical tests. The use of the short transverse (ST) tensile test is now an integral part of the specification of steels for some critical applications, particularly offshore structures (Ref. 4).

However all the abovementioned techniques rely on selecting and making the best use of the available material rather than making a positive step towards the manufacture of less susceptible steel. Lamellar tearing is a special case of ductile fracture which takes place in the ST direction of rolled steel plate and it has been shown that inclusions play a major role in determining the ST ductility of low and medium strength steels (Ref. 4). An important step forward has been the correlation of inclusion parameters with mechanical properties in the ST direction, and this previous work has been based on a range of steels, many resulting from fabrication failures (Ref. 5). The present investigation has been extended to evaluate the plate yield of single ingots. It was hoped that this would provide the opportunity of examining closely the effects of variations in inclusion population within a matrix of constant composition and yield strength. The previous assessments used a variety of steels and were carried out on small samples, many of which were from casualty sources with a wide range of plate thicknesses, compositions, yield strengths, etc.

The most detailed aspect of the work has therefore been concerned with a fully silicon killed steel to BS 1501-161 in 25 mm thickness, this being a widely used grade and thickness for welded fabrications. The data obtained from the two ingot yields of steel have been compared with those from the previous work on a number of steels subjected to different deoxidation practices with consequent different dominant inclusion types, and a range of susceptibilities to lamellar tearing.

*J. C. M. FARRAR is associated with the Welding Institute, Abington Hall, Abington, Cambridge, England.*

## Materials

A large proportion of the total plate yield of two ingots of steel manufactured to specification BS 1501-161 Grade 28A and rolled to plate 25 mm thick were supplied. This is a boiler quality carbon-manganese fully silicon killed steel and specification details are included in Table 1. One ingot was manufactured and rolled by works A and the other by works B, and the samples will be referred to as the A and B plates respectively, throughout the paper. The dimensions of the plates, and their positions in the original ingots are given in Fig. 1. Ingot A was a nominal 20 metric ton ingot whereas ingot B was a nominal 15 metric ton. In both cases the ingots were reported to be a random selection from normal production casts and were teemed into plate molds. Top pouring was used in both cases and hot tops were employed to minimize the formation of pipe. After stripping, the ingots were processed in the usual way to produce plate 2 m in width. Chemical analyses on the top and bottom of each plate were carried out using the "Quantovac" direct reading spectrograph and these are given in Table 1.

**Table 1 — Specification for BS1501-161 and Chemical Analyses of A and B Plates**

| | Mechanical properties | | | | | | | | | |
|---|---|---|---|---|---|---|---|---|---|---|
| | Yield stress, N/mm² | ksi | Tensile stress, N/mm² | | ksi | | | Elongation, % 5.65 A | | |
| Specification | 230 | 33.4 | 430-516 | | 62.4-74.8 | | | 25 | | |
| | Chemical analyses | | | | | | | | | |
| | C | Mn | Si | S | P | Ni | Cr | Mo | Cu | Al |
| BS1501-161 | 0.25 | 0.55- | 0.1- | 0.05 | 0.05 | 0.30 | 0.25 | 0.10 | 0.20 | — |
| Specification | max | 1.20 | 0.35 | max | max | max | max | max | max | — |
| A plates: | | | | | | | | | | |
| T 404C/2A | 0.25 | 0.66 | 0.14 | 0.013 | 0.006 | 0.02 | 0.03 | 0.01 | 0.02 | <0.005 |
| T 404C/2F | 0.25 | 0.67 | 0.15 | 0.015 | 0.007 | 0.02 | 0.03 | 0.01 | 0.02 | <0.005 |
| M 780C/1A | 0.25 | 0.66 | 0.15 | 0.013 | 0.006 | 0.02 | 0.03 | 0.01 | 0.02 | <0.005 |
| M 780C/1E | 0.22 | 0.66 | 0.15 | 0.013 | 0.006 | 0.02 | 0.03 | 0.01 | 0.02 | <0.005 |
| B 633C/3A | 0.20 | 0.66 | 0.15 | 0.016 | 0.006 | 0.02 | 0.03 | 0.01 | 0.02 | <0.005 |
| B 633C/3D | 0.19 | 0.66 | 0.15 | 0.013 | 0.006 | 0.02 | 0.03 | 0.01 | 0.02 | <0.005 |
| B plates: | | | | | | | | | | |
| T J406/8 | 0.17 | 0.90 | 0.14 | 0.034 | 0.041 | 0.04 | 0.03 | 0.01 | 0.03 | <0.005 |
| T J406/4 | 0.21 | 0.90 | 0.14 | 0.032 | 0.043 | 0.04 | 0.03 | 0.01 | 0.03 | 0.005 |
| M J402/1 | 0.19 | 0.88 | 0.14 | 0.033 | 0.041 | 0.04 | 0.03 | 0.01 | 0.03 | <0.005 |
| M J402/6 | 0.19 | 0.90 | 0.14 | 0.037 | 0.041 | 0.04 | 0.03 | 0.01 | 0.03 | 0.005 |
| B J401/8 | 0.18 | 0.89 | 0.14 | 0.030 | 0.042 | 0.04 | 0.03 | 0.01 | 0.03 | 0.005 |
| B J401/3 | 0.17 | 0.88 | 0.14 | 0.031 | 0.038 | 0.04 | 0.03 | 0.01 | 0.03 | 0.006 |

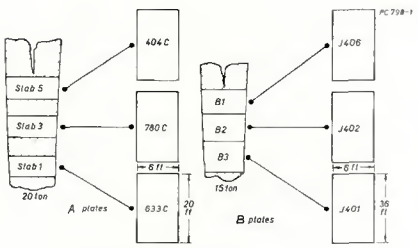


*Fig. 1 — Plate identification and positions*

## Mechanical Testing

### Background

The experimental approach consisted of determining the ST properties of samples of the plate yield of both ingots using the ST tensile and notched bend tests (Ref. 5). The two tests were chosen, since the simple ST tensile test extracted from the plate thickness without any extensions samples the region towards the plate midthickness and allows a rapid survey to be made (Fig. 2a), while the bend test samples preselected plate surface regions (Fig. 2b) and enables the inclusion data to be linked to mechanical properties for a well defined area.

### ST Tensile Tests

Samples for the ST tensile tests were extracted systematically to cover plate centers and edges from all three plates from both ingots. Certain sampling positions were adjusted to correspond to "defect" areas located during an ultrasonic survey which is not considered further in this paper. It was thought that this was the best approach for a rapid initial survey of the plates in order to locate plate areas having widely different ST properties.

The sampling positions are shown in Fig. 3, and from each area six ST tensile specimens were extracted to Hounsfield No. 14 dimensions with a 6.4 mm diameter but with a reduced gage length. Specimens were pulled to failure and reduction in area (RA) values were measured directly from the fractured specimens. Tensile strength, lower yield stress and elongation were also obtained, but RA has been found to correlate most closely with susceptibility to tearing and only these results are considered in this paper. The mean and range for the six tests from each sample are shown in Fig. 4.

The objective of this extensive survey of ST properties using the tensile test was to discover whether variations existed both within and between the two ingot plate yields. The results summarized in Fig. 4 show that ingot A generally gave high % RA values with means for the three plates of 32, 31 and 29%. Sample means showed a wider range extending from 21 to 30%. In contrast, ingot B gave significantly lower results with a much wider range of values. The plate means were 25, 23 and 15% with sample means ranging from 28 to 10%. The ST % RA values are summarized in Table 2. All the fractured specimens were preserved for subsequent examination and the results of this aspect of the investigation are described in the section on fractography.

### ST Notched Bend Test

In this test (Ref. 5) a complete through thickness sample of steel is welded between extension pieces so that a specimen can be extracted for testing in three point bending. It is possible to position the notch on any plane through the thickness so that crack initiation and propagation take place in a direction parallel to the plate surface. In this investigation the notch was placed 5 mm from the plate surface just outside the visible HAZ to assess the region in which lamellar tearing commonly occurs. The method of preparation of the testpiece and its dimensions are given in Fig. 2b. One major objective of this aspect of the work was to obtain mechanical test data and metallographic data from immediately adjacent samples so that close comparisons could be made between two assessments. For this reason alternate specimens from each sample were tested, with the remainder being retained for quantitative metallography.

Two of the samples from A ingot and five from B were selected for this aspect of the work. The specimens were tested in slow three point bending. Crack opening displacement (COD) was measured using a clip gage positioned across the notch faces. For each test a trace of force versus clip gage displacement (Vg) was obtained and from each force/Vcg curve the following data (Ref. 5) was extracted (Fig. 5).

- $\alpha$ = Vg to first attainment of maximum load, this being considered to represent a measure of resistance to initiation of lamellar tearing.
- $\beta$ = Vcg to the point of first fall-off of maximum load.
- $\gamma$ = Vcg to the point during tear

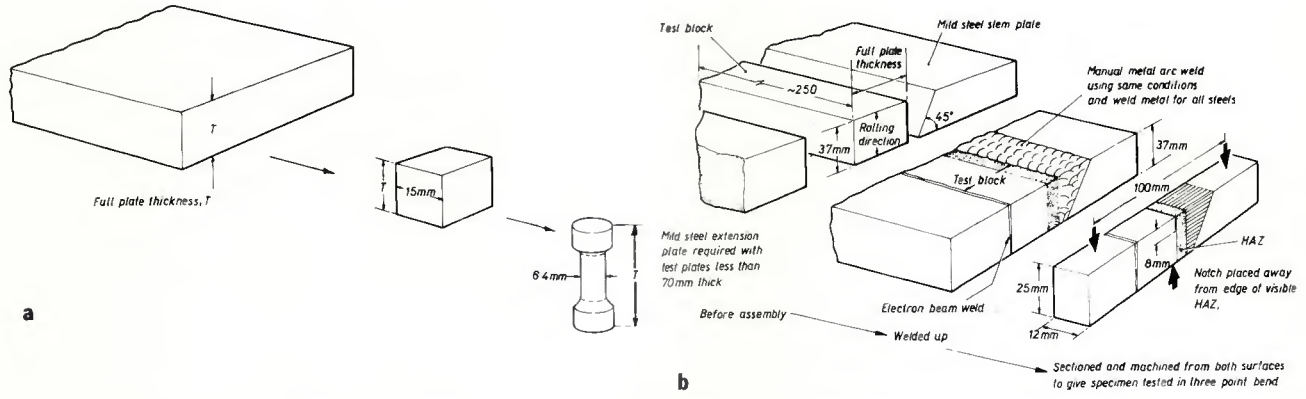


*Fig. 2 — (a) Method of extraction of ST tensile test specimen. (b) Method of extraction of ST notched bend test specimen*

propagation when the applied force was half the maximum force attained.

$\gamma - \beta$ = This was calculated to give a comparative measure of resistance to crack propagation through the specimen ligament.

A = The total area under the curve. This represents the work done in initiating a lamellar tear from a fatigue cracked notch and propagating it through the remaining ligament of the specimen. This comparison between specimens was considered valid since all the samples taken from various plates showed little variation in yield stress.

From the above data three criteria ($\alpha, \gamma - \beta, A$) were considered and the mean and spread of results for each sample are shown in Fig. 6. In order to avoid cleavage crack initiation and propagation in B steel which occurred in the bend tests carried out at room temperature (+20 C) it was found necessary to carry out some further tests at +250 C to ensure a ductile fracture mechanism. One sample from A steel was used to give a comparison between both test temperatures. At +250 C the propagation of cracking was significantly affected by dynamic strain aging and for this reason the criterion used for assessment of results from all the samples tested at both temperatures was that of COD to maximum load ( $\delta$ max), which was calculated from Vg using the relationship

$$\delta \text{ max} = \frac{Vg}{1 + r\left(\frac{a + z}{W - a}\right)}$$

where a is the total crack length, W the specimen width, z the knife edge thickness and r the rotational factor assumed to be 1/3 for the present specimen geometry. The results from

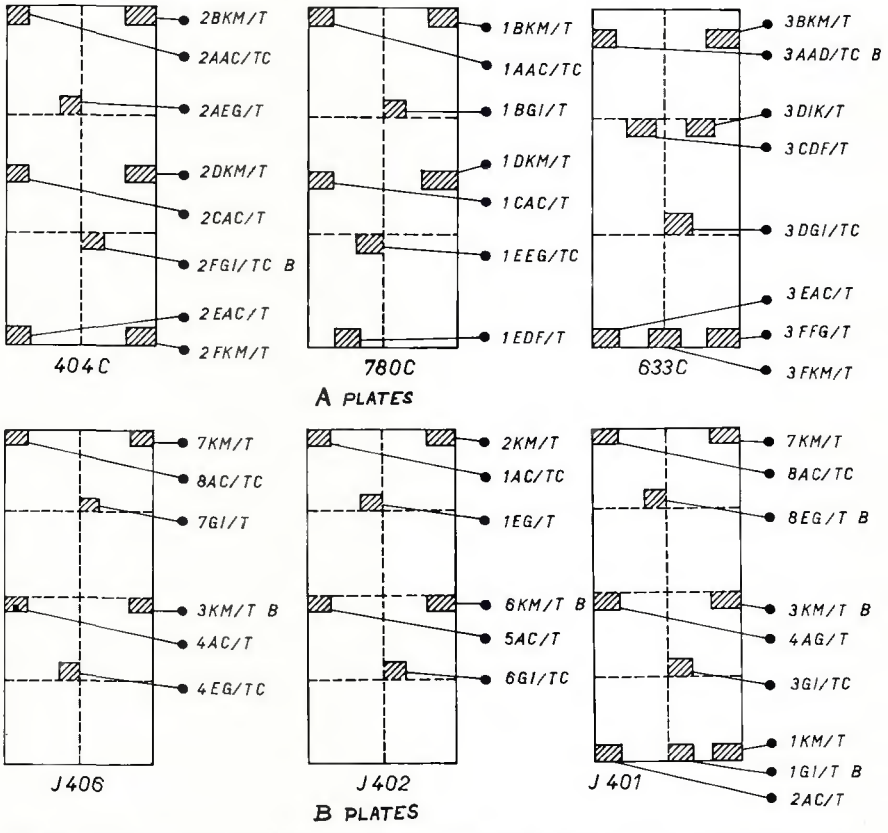


*Fig. 3 — Position within plates of testpieces: T — tensile tests; C — chemical analysis; B — bend tests*

**Table 2 — Summary of Short Transverse Percent Reduction in Area (ST % RA) from A and B Ingot Yields of Plate**

| A Steel | Overall mean % RA | Max sample mean % RA | Min sample mean % RA | Max result % RA | Min result % RA |
|---|---|---|---|---|---|
| Top plate | 32 | 39 | 21 | 43 | 16 |
| Middle plate | 31 | 38 | 26 | 43 | 18 |
| Bottom plate | 29 | 35 | 24 | 37 | 19 |
| B Steel | | | | | |
| Top plate | 25 | 28 | 22 | 38 | 10 |
| Middle plate | 23 | 27 | 20 | 46 | 8 |
| Bottom plate | 15 | 26 | 10 | 40 | 8 |

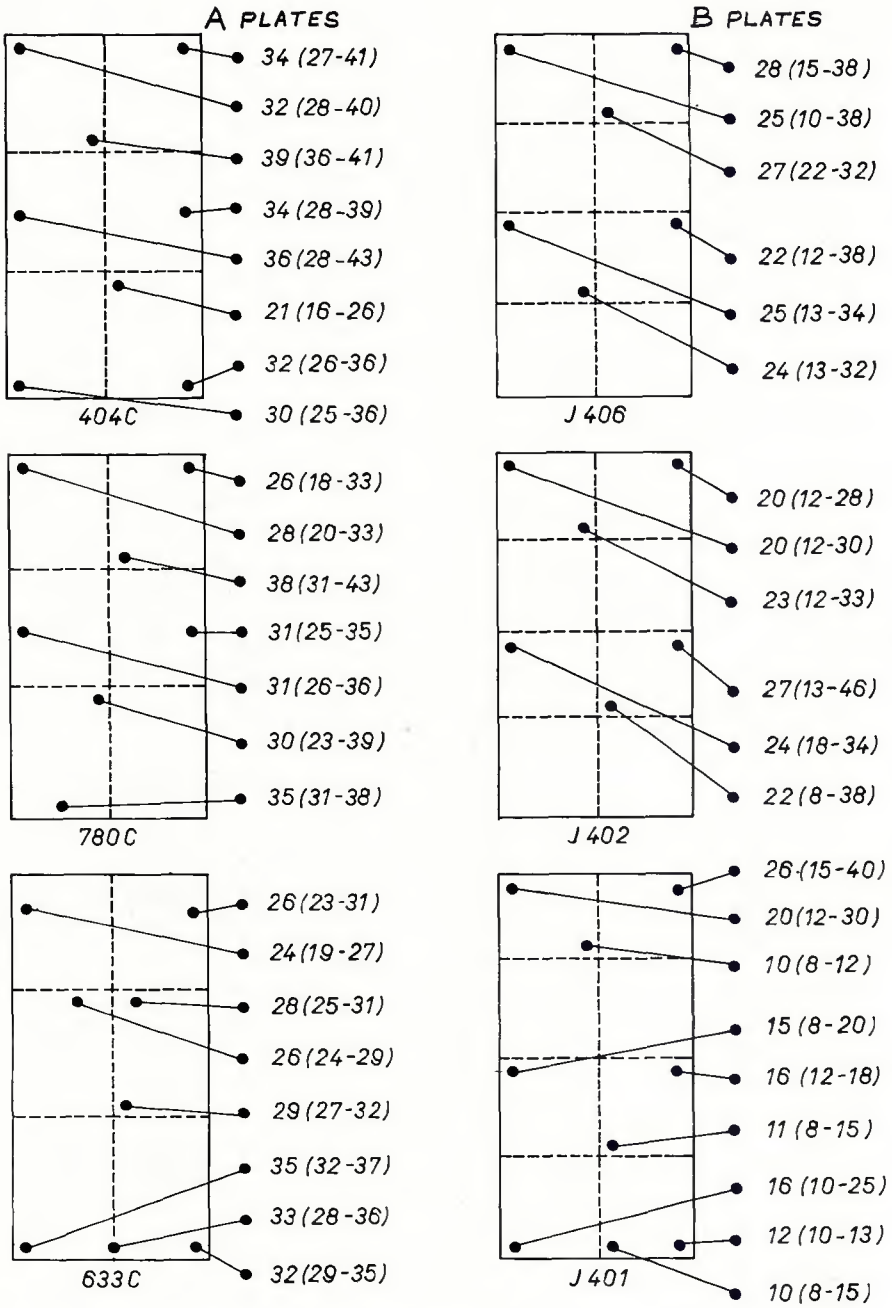


*Fig. 4 — Short transverse % RA values (mean + range)*

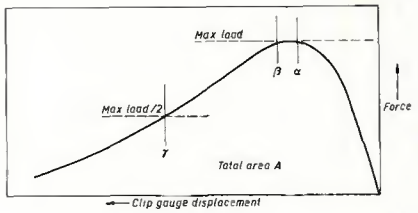


*Fig. 5 — Typical ST notched bend test force/displacement curve*

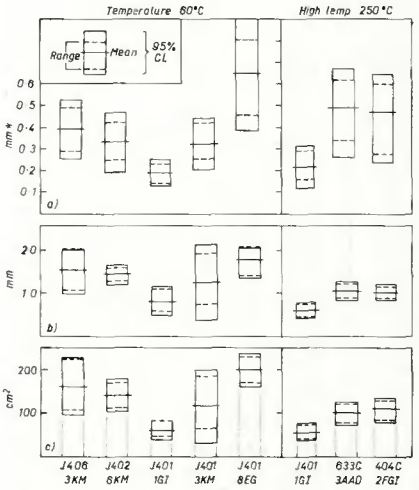


*Fig. 6 — Summary of bend test results. (a) Initiation criterion $\alpha$; (b) propagation criterion $\alpha$-$\beta$; (c) combined criterion A. These COD results are quoted as clip gage displacements*

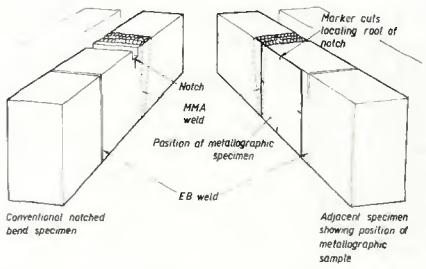


*Fig. 7 — Extraction of specimens for inclusion assessment*

the various samples exhibited a range of behaviors but the rankings did not necessarily correspond to those based on ST % RA values; it is considered that this reflects differences in potential susceptibility extending from the surface to the plate midthickness regions.

## Quantitative Metallography

### Results from Ingots A and B

In an attempt to achieve a close correlation between a metallurgical parameter and susceptibility to lamellar tearing, automatic inclusion assessments were carried out on polished sections using a Quantimet 720 Image analyzing computer (Ref. 6). In order to sample areas as close as possible to the fracture plane in the above bend tests, specimens were extracted adjacent to each bend specimen as shown in Fig. 7. The position of the base of the notch was marked on each specimen so that the polished areas to be assessed could be located as accurately as possible. Specimens were polished to give a scratch-free surface.

A number of random areas of the same plate were polished, marked, preserved with lacquer and used as a continuous standard. One of these, shown in Fig. 8, illustrates a fairly typical inclusion population. The standard area was used for equipment calibration and to apply a continuous correction to compensate for equipment drift.

The sensitivity of the detection system was set to assess inclusions greater than 1-2$\mu$m in diameter (i.e., all those visible in Fig. 8). No attempt was made to distinguish between inclusion types since previous work had shown that all the common types of inclusion can participate in the lamellar tearing process (Ref. 5). Two parameters were assessed, these being:

1. The volume fraction of inclusions (Vf). This is numerically the same as the area fraction on a random plane through the volume (Ref. 7) and is often taken as a measure of overall cleanness.

2. The projected length of inclusion (P). This is a fundamental parameter which enables an assessment of an array of non-spherical particles to be made. The total length of inclusions parallel to the rolling direction in any one field is measured and it has been shown that this parameter is related to three important inclusion variables — volume fraction, size and shape (Refs. 5,8). The projected length parameter (P) is inversely proportional to the inter-inclusion spacing in the most likely direction of fracture and so would be expected to bear some direct relationship with susceptibility to lamellar tearing.

The mean volume fractions (Vf) and projected length per unit area (P) for each sample are given in Table 3. These have been computed from the total array of 200 fields/specimen.

It is possible that a relationship exists between susceptibility to tearing, as assessed by one or more of the bend test parameters, and one or both of the inclusion assessment parameters. This correlation might exist at a number of levels. Firstly, between any individual bend test and the corresponding metallographic section. Secondly, between samples covering a range of levels from both bend tests and metallographic sections for the BS 1501-161 steel described. Thirdly, between mechanical test results and inclusion assessments taken from a range of structural steels. The first two relationships will be considered here; the third will be dealt with in the next section when the results from a wider range of steels are introduced.

Within a group of results from each sample there was no evidence of a well-defined relationship between individual bend test results and the corresponding inclusion assessment. This apparent discrepancy probably arises because of the problems of estimating the inclusion population participating in the fracture of a bend test specimen.

Ideally the inclusion population of the fracture surface is the most relevant and there may be wide variations between this population and an adjacent one from a polished section. However when the sample means are considered it is found that there is a correlation between increasing susceptibility to tearing as assessed by the bend test and the inclusion assessment parameters. The best defined relationship exists between COD to initiation ( $\delta$ max) and inclusion projected length (P), as shown in Fig. 9a. The corresponding relationship with inclusion volume fraction (Vf) is shown in Fig. 9b, and it can be seen that there is significantly more scatter.

**Results from All Steels**

The detailed results in the above section only apply to one type of steel (silicon killed) and only cover a relatively small range of results. It is probable that these results do not extend over the extremes of steel cleanness and in order to put them in perspec-

*Fig. 8 — Typical array of inclusions used for calibration*

**Table 3 — Summary of Inclusion Population Data for Samples Evaluated with the Bend Test**

| Code | Plate | Mean Inclusion Projection $m \cdot \mu^{-1} \times 10^3$ | Mean Inclusion Volume % |
|---|---|---|---|
| 633C/3A | A Bottom | 0.98 | 0.26 |
| 404C/2F | A Top | 1.10 | 0.31 |
| J406/3 | B Top | 1.40 | 0.48 |
| J402/6 | B Middle | 1.21 | 0.40 |
| J401/1 | B Bottom | 1.95 | 0.52 |
| J401/3 | B Bottom | 1.28 | 0.37 |
| J401/8 | B Bottom | 1.12 | 0.38 |
| J401/1 | B Bottom | 1.90 | 0.54 |

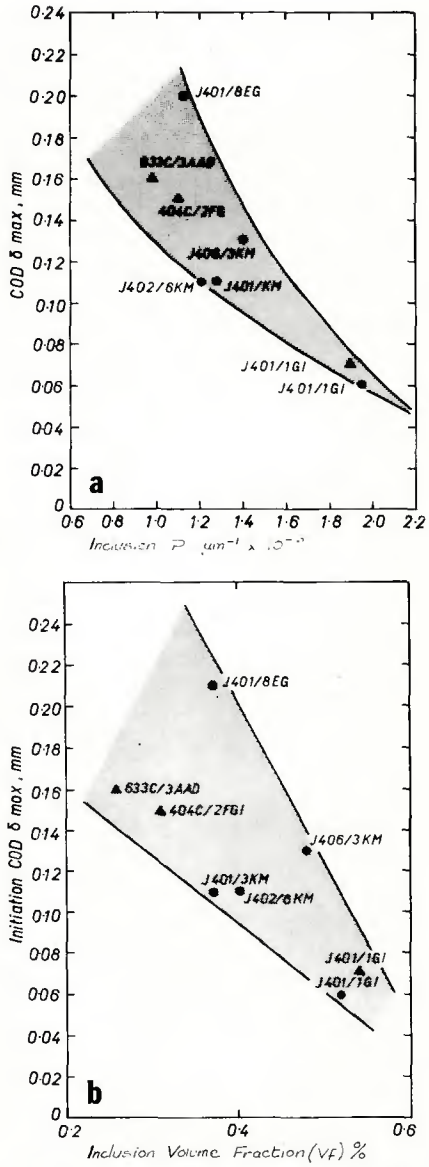


*Fig. 9 — (a) Plot of bend test COD ( $\delta$ max) versus inclusion projected length (P) based on sample means. (b) Plot of bend test COD ( $\delta$ max) versus inclusion volume fraction (Vf) based on sample means*

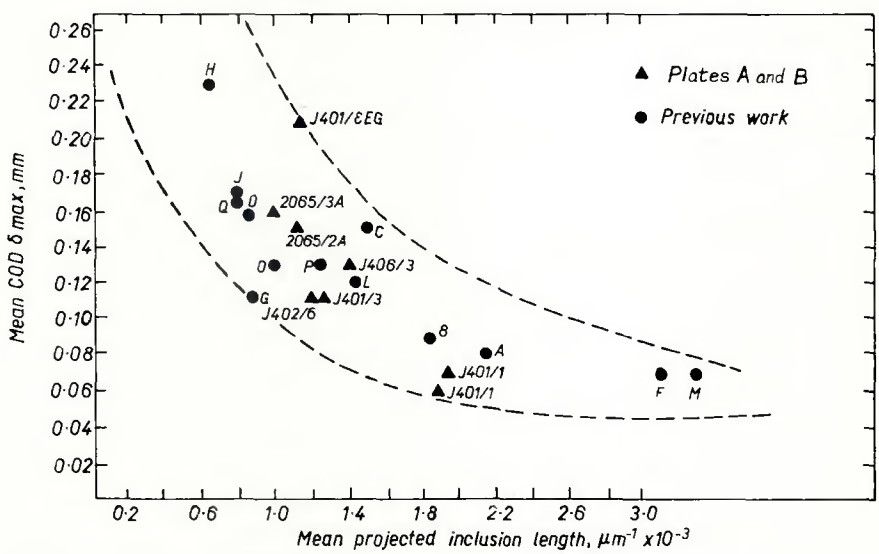


*Fig. 10 — Plot of $\delta$ max versus P for all steels*

**Table 4 — Details of Steels Used in this Investigation**

| Code | Specification | Thick-ness, mm | Composition as analyzed C | Mn | Si | S | P | Al[(a)] | $O_2$[(a)] | Others[(a)] | Material history[(b)] |
|---|---|---|---|---|---|---|---|---|---|---|---|
| A | HSB 50 | 12 | 0.19 | 1.58 | 0.45 | 0.023 | 0.021 | 0.042 | 0.001 | — | Fab failure |
| B | HSB 50 | 15 | 0.19 | 1.40 | 0.37 | 0.024 | 0.018 | 0.048 | 0.001 | — | Fab failure |
| C | B.S. 15 | 57 | 0.21 | 0.82 | 0.16 | 0.035 | 0.017 | — | 0.028 | — | Test failure |
| D | Admiralty 'B' | 32 | 0.15 | 1.35 | 0.25 | 0.025 | 0.021 | 0.038 | 0.004 | — | Reported |
| F | B.S. 968 | 12 | 0.14 | 1.54 | 0.31 | 0.028 | 0.022 | 0.038 | 0.002 | — | Fab failure |
| G | B.S. 968 | 32 | 0.19 | 1.50 | 0.03 | 0.043 | 0.037 | — | — | 0.12Cr 0.034Nb | Unknown |
| H | B.S. 1501-161 | 51 | 0.12 | 0.55 | 0.18 | 0.045 | 0.034 | — | 0.010 | — | Unknown |
| J | B.S. 1501-151 | 51 | 0.19 | 0.71 | 0.02 | 0.025 | 0.022 | — | 0.011 | — | Unknown |
| L | Lloyds E | 32 | 0.15 | 1.20 | 0.12 | 0.021 | 0.011 | 0.056 | 0.002 | — | Reported |
| M | Unknown | 32 | 0.24 | 1.53 | 0.27 | 0.037 | 0.018 | 0.010 | 0.002 | — | Reported |
| O | B.S. 1501-151 | 41 | 0.23 | 0.70 | 0.03 | 0.034 | 0.006 | — | — | 0.1Ni, 0.04Cr, 0.01Mo | Reported |
| P | B.S. 1501-221 | 44 | 0.17 | 1.27 | 0.22 | 0.034 | 0.021 | — | — | 0.1Ni, 0.05Cr, 0.025Mo | Unknown |
| Q | B.S. 1501-211 | 51 | 0.15 | 1.18 | 0.01 | 0.036 | 0.016 | — | — | 0.05Ni, 0.02Cr, 0.02Mo | Unknown |

(a) A dash indicates that no analysis was carried out
(b) Comments on material history:
Fab failure — Sample from fabrication failure with evidence of lamellar tearing present
Test failure — Sample which exhibited lamellar tearing in laboratory welding test
Reported — Sample from the same plate as a reported failure caused by lamellar tearing
Unknown — Pedigree material which has never been incorporated into a fabrication

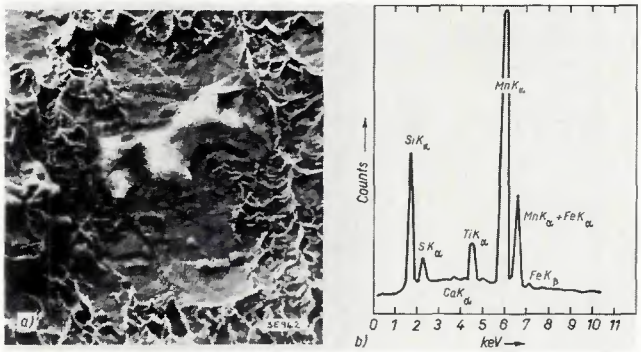


*Fig. 11 — Typical large silicate inclusion with analysis trace — scanning electron micrograph (SEM); X 300, reduced 53%*

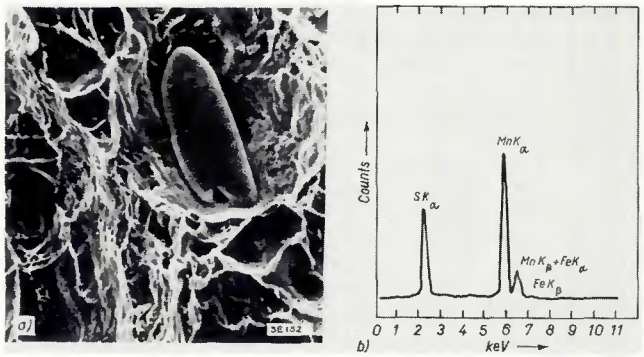


*Fig. 12 — Typical Type I MnS inclusion with analysis trace — SEM; X700, reduced 53%*

**Table 5 — Summary of Inclusion Data and Bend Test δ max Values for Steels in this Investigation**

| Code | Mean inclusion Projection $\mu m^{-1} \times 10^3$ | Volume, % | Mean δ max, mm |
|---|---|---|---|
| A | 2.15 | 0.42 | 0.08 |
| B | 1.85 | 0.34 | 0.09 |
| C | 1.50 | 0.49 | 0.15 |
| D | 0.83 | 0.18 | 0.16 |
| F | 3.10 | 0.50 | 0.07 |
| G | 0.85 | 0.24 | 0.11 |
| H | 0.63 | 0.19 | 0.23 |
| J | 0.78 | 0.19 | 0.17 |
| L | 1.43 | 0.31 | 0.12 |
| M | 3.28 | 1.04 | 0.07 |
| O | 0.98 | 0.39 | 0.13 |
| P | 1.23 | 0.34 | 0.13 |
| Q | 0.78 | 0.23 | 0.17 |

tive they have been compared with those from a range of steels produced using different deoxidation practices and some having a history of lamellar tearing. The details of these steels are given in Table 4, including those from Ref. 5.

The bend test δ max values and corresponding inclusion assessment data are given in Table 5. All the results of δ max versus P are shown in Fig. 10, and they indicate a marked trend of increasing susceptibility to tearing with increasing inclusion content. Since a number of different inclusion types were involved in the fracture process (Table 6), it appears that the relationship between δ max and P is largely independent of inclusion type. This implies that dense clusters of highly elongated inclusions or elongated fragmented particles are detrimental from the lamellar tearing point of view irrespective of whether they are elongated Type II manganese sulfides, manganese silicates or alumina particles.

## Fractography

### Results from Ingots A and B

From each sample of the two ingot yields investigated, the fracture surfaces of the highest and lowest ST % RA values were selected for detailed fractographic examinations in the scanning electron microscope (SEM). On each specimen the following observations were made:

1. The overall fracture appearance, i.e., degree of roughness, approximate size of microvoids, etc.
2. The approximate length of the largest inclusions present.
3. The qualitative chemical analysis of the inclusions present using a rapid energy dispersive x-ray analysis system attached to the SEM.

Three major inclusion types were

identified from the two ingot yields of plate; namely, complex manganese silicates (Fig. 11), manganese sulfides generally of the Type I form (Fig. 12), and duplex silicate/sulfide inclusions (Fig. 13). Within this broad classification there existed a wide range of inclusion sizes from ~10 $\mu$m in diameter to 5 mm in length. In addition it was also found possible to grade inclusions in terms of distribution ranging from single isolated to close packed.

It appears that the RA values resulting from ST tests are highly dependent upon the maximum size of inclusion present within the gage length with smaller close packed inclusions behaving in much the same way as large isolated inclusions. The evidence for this relationship is shown in Fig. 14, which illustrates the effect of inclusion type, size and distribution upon measured ST % RA values. This is not a definitive quantitative relationship, but an indication of the trends which are apparent from the observations during fractography. It does however, confirm earlier observations carried out on higher strength quenched and tempered steels (Ref. 9).

Figure 14 is also important in emphasizing the effects of inclusion type upon susceptibility to lamellar tearing. It shows that silicate inclusions dominate specimens with RA values below 15%, the levels appropriate to maximum lamellar tearing risk, whereas manganese sulfide inclusions of the Type I give rise to RA values of greater than 30%,

**Table 6 — Summary of Inclusion Populations and Maximum Sizes from Steels Used in this investigation**

| Code | Thickness, mm | Deoxidation practice | Material history[a] | Max inclusion length, $\mu$m | Predominant inclusion type | Others |
|---|---|---|---|---|---|---|
| A | 12 | Fully killed + Al | Fab failure | 700 | Highly elongated MnS (Type II) | |
| B | 15 | Fully killed + Al | Fab failure | 500 | Highly elongated MnS (Type II) | |
| C | 57 | Fully killed | Test failure | 2000 | Elongated silicates and duplex inclusions | Number of broken silicates and undeformed MnS |
| D | 32 | Fully killed + Al | Reported | 250 | Elongated MnS (Type II) | Silicate stringers $Al_2O_3$ particle stringers |
| F | 12 | Fully killed + Al | Fab failure | 1000 | Highly elongated MnS (Type II) | |
| G | 32 | Semikilled + Nb | Unknown | 700 | Deformed silicates | Some MnS |
| H | 51 | Vac. deoxidized | Unknown | 150 | Slightly deformed and some elongated MnS (Type II) | |
| J | 51 | Semikilled | Unknown | 1000 | Moderately deformed silicates, sulfides and duplex | Number of broken inclusions |
| L | 32 | Fully killed + Al | Reported | 750 | Elongated MnS (Type II) | $Al_2O_3$ particle stringers |
| M | 32 | Unknown | Reported | 5000 | Highly deformed MnS (Type II) | |
| O | 41 | Semikilled | Reported | 500 | Silicates and MnS (Type II) | |
| P | 44 | Fully killed | Unknown | 600 | Elongate silicates | |
| Q | 51 | Semikilled | Unknown | 100 | Slightly deformed MnS (Type I) | |

(a) See Table 4

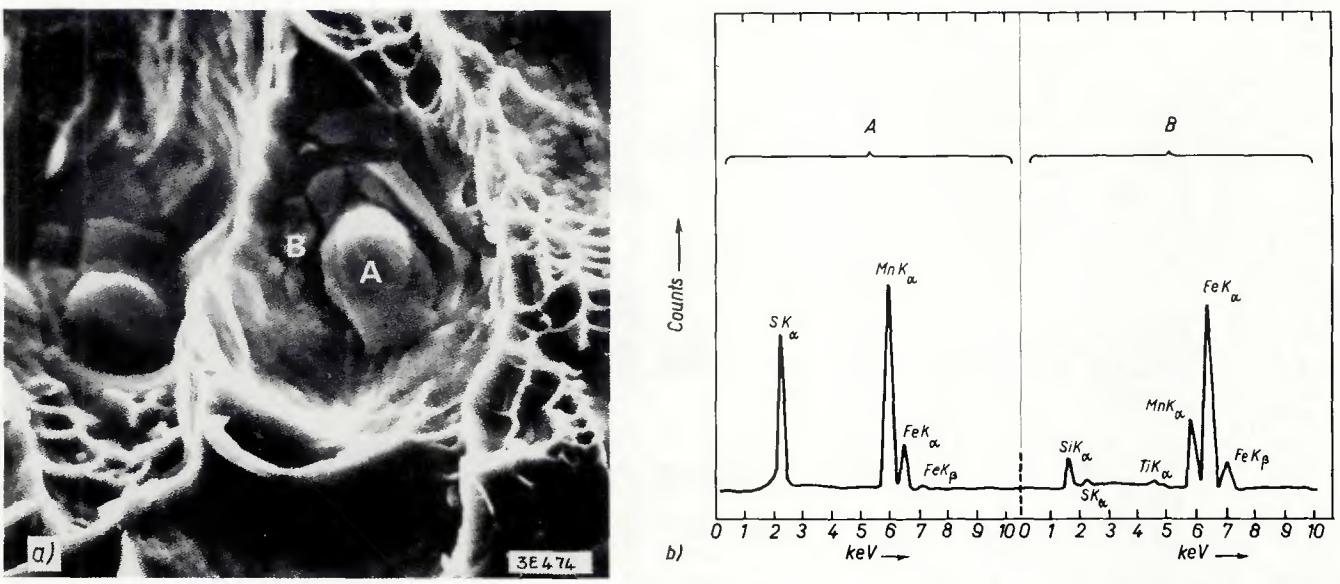


*Fig. 13 — (a) Typical duplex inclusion with globular Type I MnS and fractured silicate surround — SEM; X2000, reduced 14%. (b) Analysis trace*

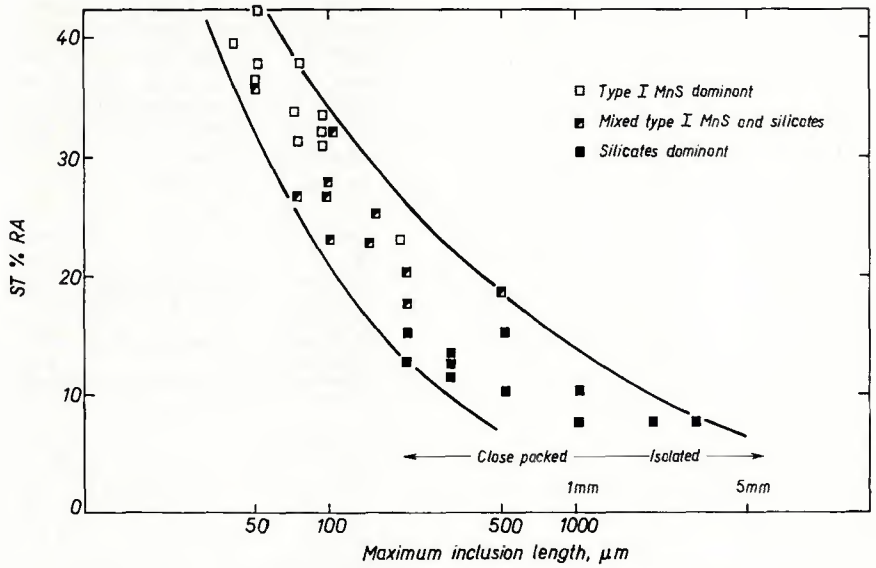


*Fig. 14 — Relationship between inclusion type, size, distribution and ST % RA for ingot steels A and B*

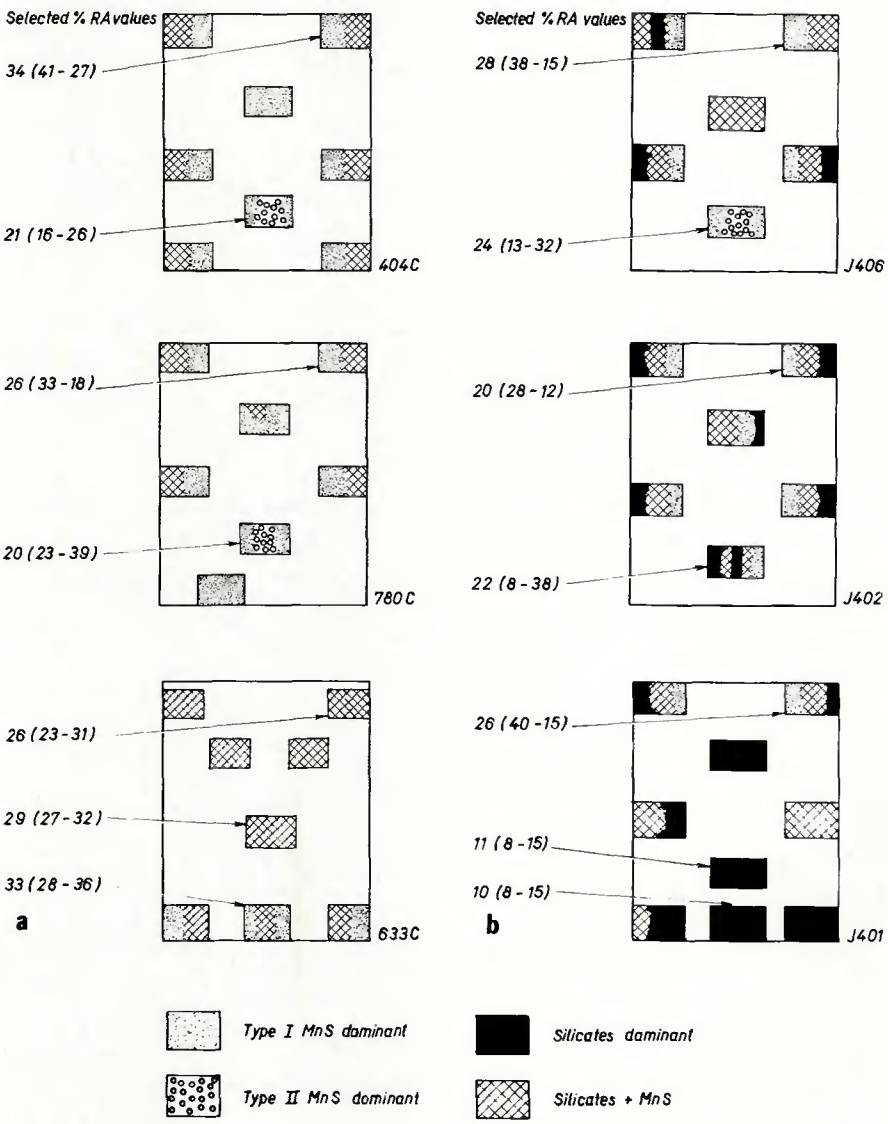


*Fig. 15 — (a) Schematic distribution of inclusion types within A plates. (b) Schematic distribution of inclusion types within B plates. (Not to scale — each area approximately 300mm²)*

which are considered "safe" from lamellar tearing (Ref. 4).

Having established the inclusion types present on the fracture surfaces and obtained the correlations with susceptibility to tearing, it is appropriate to map out the distribution of the major inclusion types within the plates from the two ingot yields. These are shown in Fig. 15. It can be seen that there is a wide variation in the plates from A which corresponds to the wide range of ST properties. The dominance of large silicate inclusions in the bottom plate resulted in a large number of low % RA specimens and also the notched bend specimens with the lowest $\delta$ max values. The distribution of the large silicates in the bottom plate is consistent with the occurrence of a "bottom cone" of inclusions in this region (Refs. 10,11). In the B plates the inclusion population is generally more uniform with silicate inclusions not dominating any of the areas sampled. This fact is reflected in the consistently high ST % RA values (~30%).

It should be noted in samples towards the upper plate centerlines of both steels, A and B, that MnS inclusions with a Type II format were identified. Although these are not commonly found in semi-killed and fully silicon killed steels of the type described in this paper, they are often the dominant inclusion type found in aluminum treated killed steels and are discussed in the next section.

**Results from Other Steels**

Fractographic investigations have been carried out on a wide range of steel types (Table 6). In the same way that the relationship between bend test parameters and inclusion projected length has been found to be independent of inclusion type, so the relationship between inclusion size and ST % RA has also been found to be independent of inclusion type.

Figure 16 summarizes the inclusion length measurements from a range of steels in relation to the ST % RA values. It can be seen that the basic transition from silicates to Type I MnS inclusions as the RA values increase is still maintained, but it is most important to note that a similar transition takes place from Type II MnS to Type I MnS. In practical terms this means that Type II MnS which arises in aluminum treated fully killed steels (Fig. 17) can be just as detrimental to ST properties as gross clusters of elongated silicate inclusions. In fact, because they can be evenly distributed across large areas of plate and clustered on selected planes through the thickness, rather than segregated in fairly discrete regions in a plate, they are potentially more of a problem and can give rise

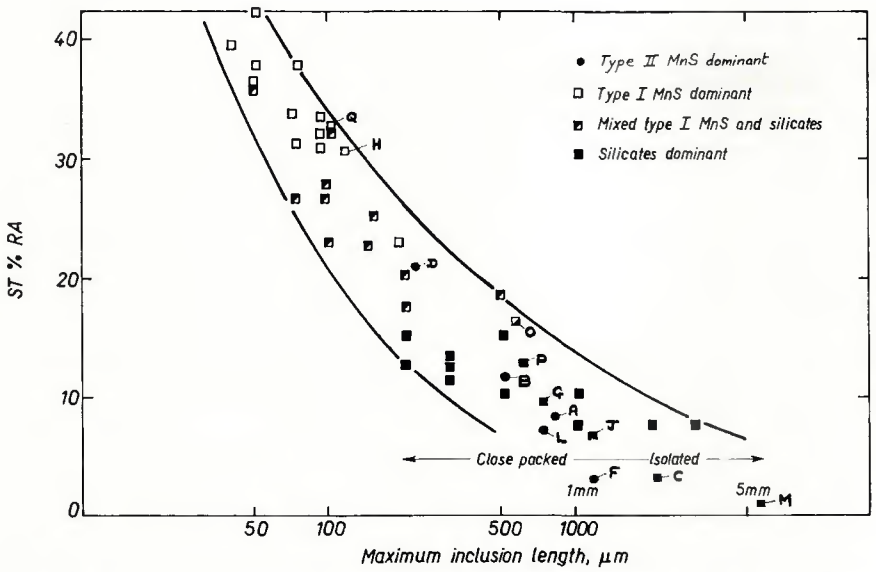


*Fig. 16 — Relationship between inclusion type, size, distribution and ST % RA for all steels*

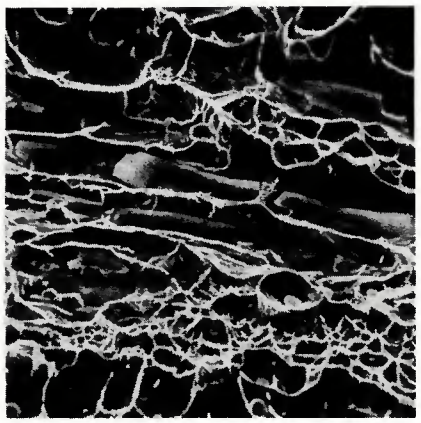

*Fig. 17 — ST tensile test fracture surface from A top plate (16% RA) showing thin tape-like Type II MnS inclusions (SEM)*

to very extensive lamellar tearing.

Aluminum oxide stringers often arise in conjunction with Type II MnS inclusions in aluminum treated steels (Fig. 18). In an isolated specimen they can dominate the fracture surface and the same inclusion length/ST % RA relationship holds good, but distribution throughout steel plates is not uniform and they seldom give rise to extensive lamellar tearing problems in isolation from other inclusion types.

ST tensile specimens are therefore sensitive to large single inclusions and arrays of smaller inclusion on a single plane rather than the overall distribution within the plate thickness. A measure of total inclusion population can be taken as the volume fraction and this is shown plotted against ST % RA in Fig. 19. As would be expected there is a trend of increasing ST % RA with reducing volume fractions but the relationship is not so well defined as that between maximum inclusions size and ST % RA.

The fractography of mechanical test specimens can be extended to the examination of notched bend test surfaces. These results do not appear to be so dependent upon individual size but more upon inclusion distribution as typified by the inclusion projected length parameter P. However the same transitions of inclusion type can be observed with increasing susceptibility to tearing as monitored by the ST notched bend tests and the summary of results from ingot steel A is shown in Fig. 20.

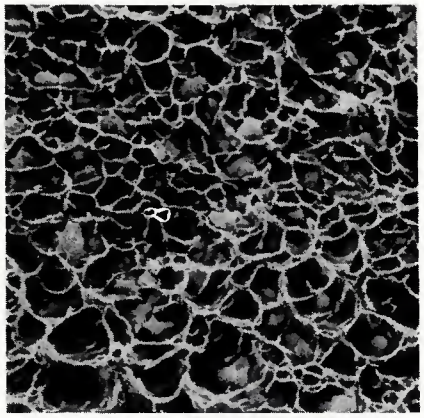

*Fig. 18 — Aluminum oxide inclusions, (SEM) X680, reduced 46%*

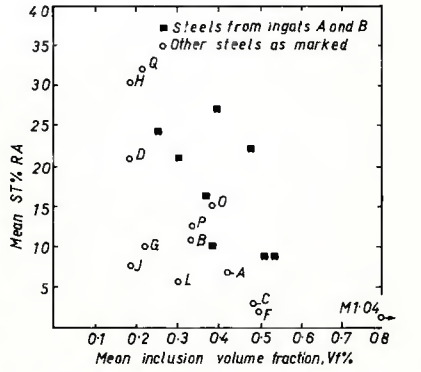


*Fig. 19 — Plot of ST % RA versus inclusion volume fraction for all steels*

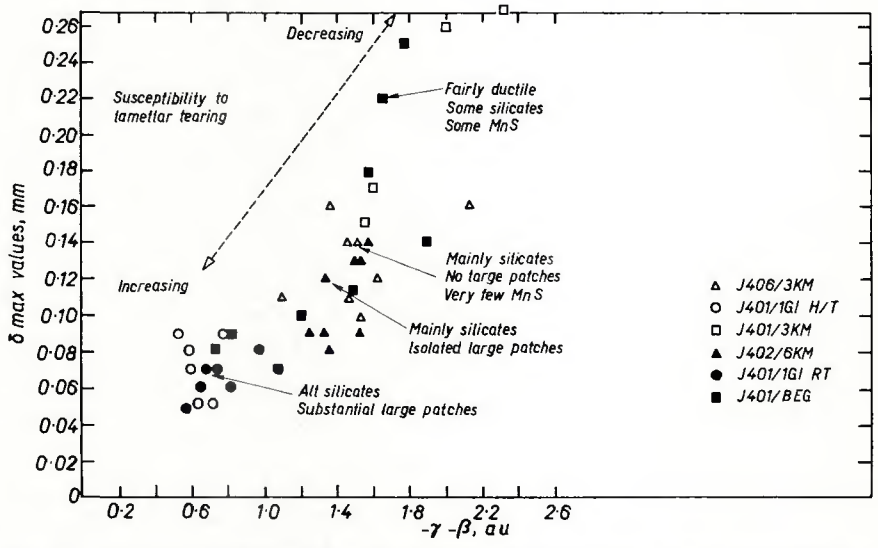


*Fig. 20 — Summary of bend test data for ingot steel A showing increase in susceptibility to tearing with change in inclusion type*

## General Discussion — the Practical Implications

Two distinct investigations have been carried out. The first was a quantitative study into the relationship between ST mechanical properties and an inclusion assessment parameter which is independent of inclusion type. The second was a qualitative study into the types of in-

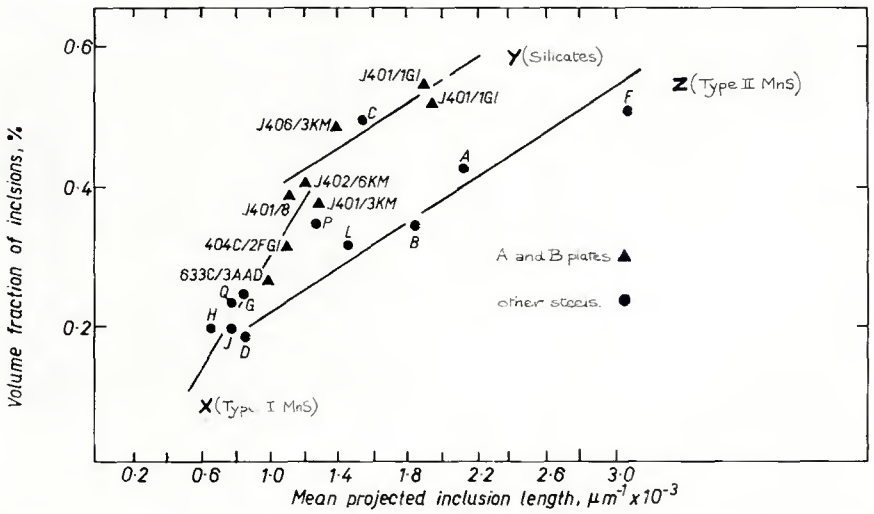


*Fig. 21 — Plot of mean inclusion projected length versus mean volume fraction for all steels*

clusions present on fracture surfaces and their relationship with the results of destructive mechanical tests from which the surfaces arose. Potentially the most valuable information arises when these two aspects of the work are combined, and a method whereby this might be carried out is suggested.

Figure 21 illustrates a plot of inclusion volume fraction versus inclusion projected length for the ingot samples and the background steels. On this plot are drawn three tentative relationships X, Y, Z. When the fractographic information about dominant inclusion types is superimposed upon this diagram, it can be seen that line X corresponds to Type I manganese sulfides, line Y to manganese silicates and line Z to Type II MnS (these being majority inclusions present in the steels investigated). The mean projected length P axis can be considered as a measure of susceptibility to lamellar tearing: the steels with a well-defined history of tearing having P values in excess of 1.4 $\mu m^{-1} \times 10^{-3}$.

If a P value of $1.8 \mu m^{-1} \times 10^{-3}$ is chosen (typical for susceptible steels), then the corresponding volume fractions of the various inclusion types can be estimated. Line X can be extrapolated beyond the data given in Fig. 21 to give a volume fraction of Type I MnS inclusions of ~ 0.6%. To achieve the same P value, the Vf for silicate inclusions (line Y) is ~ 0.5% while that for Type II MnS inclusions is just greater than 0.3%. Lines X and Y are shown as two well defined straight line relationships whereas observations of inclusion types suggest that a continuous transition takes place between Type I MnS and silicate inclusions as the dominant type. It therefore appears that silicate inclusions are unlikely to be present as the dominant inclusion type at P values below $1.3\text{-}1.4 \mu m^{-1} \times 10^{-3}$.

The trends suggested from Fig. 21 are consistent with practical experience of lamellar tearing and the various inclusion types responsible for the tearing. In silicon killed and semikilled steels with Type I MnS inclusions and manganese silicate inclusions, the former are seldom found to be responsible for lamellar tearing problems. Silicate inclusions give rise to lamellar tearing problems but only in segregated areas of plate or dirty plates with high inclusion volume fractions (e.g., parts of bottom plate of ingot A). On the other hand, steels which have been aluminum treated, usually for grain refinement and improved toughness, have been found to contain Type II MnS as the dominant type, and these are often responsible for lamellar tearing on a very extensive scale. Susceptible steels can often arise with low volume fractions of Type II MnS inclusions provided that the projected inclusions length is sufficiently high.

Figure 21 also shows that the lines Y and Z are approximately parallel with the Type II MnS inclusions having a substantially greater P value for a given volume fraction than the manganese silicates. This is completely in agreement with observations of these two inclusion types which confirm that Type II MnS inclusions have a higher aspect rate than manganese silicates, and are generally tape-like rather than oval in shape (see Figs. 12 and 17).

It is therefore important for the steelmakers to reduce the inclusion content of the plate with particular emphasis being placed upon projected length, if susceptibility to tearing is to be minimized. The significance of the parameters P is now being recognized and strenuous efforts are being made by steel producers to reduce the incidence of tearing in steels for critical applications.

For example, very low sulphur contents are now being specified and achieved in an attempt to reduce sulfide inclusion volume fraction particularly where Type II MnS inclusions are known to be a problem. In some cases rare earth additions are made to modify inclusion shape away from the Type II form and to a globular form with a substantial reduction in P values. Control is being applied to deoxidation and ingot segregation in an attempt to avoid problems with elongated silicate inclusions and clusters of alumina particles.

It is becoming increasingly common for purchasers of large quantities of steel plate for critical applications to specify the minimum ST properties required. Tests are usually carried out using small scale ST tensile testpieces (Ref. 4) extracted in limited numbers from plate edges. Ideally such specimens should be extracted from the "worst" regions in a plate so that they correspond to the minimum ST properties likely to be found.

In order to achieve this objective it is necessary to have the information about the variations of ST % RA and inclusion populations with plate yields. Figures 4 and 15 illustrate the wide range of ST % RA values and the corresponding inclusion distribution within two ingot yields of plate. It will become increasingly important that the steel producers have similar information about steel plate to be supplied for critical applications so that objective decisions about the number and location of small scale testpieces for specification purposes can be made.

## Summary and Conclusions

Two pedigree ingots of a fully silicon killed C-Mn steel in plate form have been investigated using small scale destructive tests to assess short transverse (ST) properties. The ST tensile test was used to carry out a systematic survey of ST % RA values and to locate areas of widely differing potential susceptibility to lamellar tearing. An ST notched bend test was used to examine certain areas in more detail and to investigate susceptibility to lamellar tearing close to the plate surface.

The inclusion populations of samples immediately adjacent to the bend test samples were assessed using automatic inclusion counting, and ST tensile test specimens were examined in detail using the scanning electron microscope.

The relationships which exist between inclusion populations and

potential susceptibility to lamellar tearing have been examined and the data extended to cover a wide range of steels, some with a history of lamellar tearing. The following conclusions have been drawn:

1. An inclusion projected length parameter P which is a function of inclusion size, shape and distribution has been found to correlate well with the results of the ST bend tests, with high P values corresponding to increased susceptibility to lamellar tearing as measured by COD to maximum load ( $\delta$ max). The results from a number of steels containing a range of inclusion types fall within the same scatter band and the relationship between P and $\delta$ max is independent of inclusion type.

2. Fractographic assessments of inclusion type and size and distribution have been found to correlate with ST % RA values obtained from the tensile tests, with increasing inclusion size corresponding to a reduction in ST % RA values. It has been found that a transition in dominant inclusion types from manganese silicate to Type I MnS results in an increase in ST % RA values with the transition occurring at 15-20% RA. When further steels and additional inclusion types were considered it was found that a similar transition exists between Type II MnS and Type I MnS.

3. A distinct inclusion volume fraction, projected length relationship for each of Type I MnS, Type II MnS and manganese silicate inclusions has been suggested and considered to be consistent with fabrication experience of different steel types. In order to achieve projected length P values appropriate to lamellar tearing, very high volume fractions of Type I MnS are required, and this corresponds to the lack of lamellar tearing problems found to be associated with this type of inclusion. Silicate inclusions require a somewhat lower volume fraction and have been shown to be responsible for lamellar tearing in segregated areas of plate or extensively in plates with very high inclusion populations. Type II MNS inclusions require a still lower volume fraction to achieve the necessary P value and this is consistent with the high incidence of lamellar tearing in some fully killed aluminum treated steels where highly elongated Type II MnS inclusions are often the dominant type.

*Acknowledgements*

The author is grateful to the Welding Institute Lamellar Tearing Contract Sponsor Group for financial support of much of the above work and for permission to publish this paper. He is indebted to those organizations that supplied materials for the investigation and would like to thank colleagues at The Welding Institute for their assistance in this project.

*References*

1. *Lamellar Tearing in Welding Steel Fabrication,* The Welding Institute, 1972.

2. Farrar, J. C. M., Dolby, R. E., and Baker, R. G., "Lamellar Tearing in Welded Structural Steels," *Welding Journal,* Vol. 48 (7), July 1969, Res. Suppl. pp 274-s to 282-s.

3. Jubb, J. E. M., "Lamellar Tearing," *W.R.C. Bulletin No. 168,* Dec. 1971.

4. Farrar, J. C. M., Ginn, B. J., and Dolby, R. E., "The Use of Small Scale Destructive Tests to Assess Susceptibility to Lamellar Tearing." Paper presented at The Welding Institute Conference, *Welding in Offshore Constructions,* Feb. 1974.

5. Farrar, J. C. M., Charles, J. A., and Dolby, R. E., "Metallurgical Aspects of Lamellar Tearing," *Proc. of Conf. on Effect of Second Phase Particles on the Mechanical Properties of Steel,* The Iron and Steel Institute, 1971.

6, Fisher, C., "The New Quantimet 720," *The Microscope,* Vol. 19, Jan. 1971, p 1.

7. Underwood, E., *Quantitative Stereology,* Addison-Wesley, 1970, Reading, Mass.

8. Baker, T. J. and Charles, J. A., "Influence of Deformed Inclusions upon the Short Transverse Ductility," *Proc. of Conf. on Effect of Second Phase Particles on the Mechanical Properties of Steel,* The Iron and Steel Institute, 1971.

9. Dolby, R. E., *The Metallurgy and Welding of QT35 and HY80,* The Welding Institute. To be published.

10. Fourth Report on the Heterogeneity of Steel Ingots, *ISI Special Report 2,* 1932.

11. Dickinson, J. H. S., "A Note on the Distribution of Silicates in Steel Ingots," *JISI,* Vol. 113, 1926, pp 177-211.